The Sonic Hedgehog Pathway Stimulates Prostate Tumor Growth by Paracrine Signaling and Recaptures Embryonic Gene Expression in Tumor Myofibroblasts

Aubie Shaw[1,2,3], Jerry Gipp[2,3] and Wade Bushman[1,2,3]

[1]Department of Surgery, Division of Urology, [2]The McArdle Laboratory for Cancer Research, [3]Paul P. Carbone Comprehensive Cancer Center, University of Wisconsin, Madison, WI, 53792, USA

Please send all correspondence to:
Wade Bushman
Department of Surgery
600 Highland Ave
Madison, WI 53792
phone: (608)-265-8705
fax: (608)-265-8133
email: **bushman@surgery.wisc.edu**

short title: Myofibroblasts Direct Prostate Tumor Growth

Disclosure Statement
Aubie Shaw: no disclosures
Jerry Gipp: no disclosures
Wade Bushman: no disclosures

Grant sponsor: Department of Defense; grant number W81XWH-06-1-0060 (AS)
Grant sponsor: Department of Defense; grant number W81XWH-04-1-0263 (WB)
Grant sponsor: National Institutes of Health; grant number DK056238-06 (WB)

ABSTRACT

The Hedgehog (Hh) pathway contributes to prostate cancer growth and progression. The presence of robust Shh expression in both normal prostate and localized cancer challenged us to explain the unique growth promoting effect in cancer. We show here that paracrine Hh signaling exerts a non-cell autonomous effect on xenograft tumor growth and that Hh pathway activation in myofibroblasts alone is sufficient to stimulate tumor growth. Nine genes regulated by Hh in the mesenchyme of the developing prostate were found to be regulated in the stroma of Hh over-expressing xenograft tumors. Correlation analysis of gene expression in matched specimens of benign and malignant human prostate tissue revealed a partial 5 gene fingerprint of Hh-regulated expression in stroma of all cancers and the complete 9 gene fingerprint in the subset of tumors exhibiting a reactive stroma. No expression fingerprint was observed in benign tissues. We conclude that changes in the prostate stroma due to association with cancer result in an altered transcriptional response to Hh that mimics the growth promoting actions of the fetal mesenchyme. Patients with an abundance of myofibroblasts in biopsy tissue may comprise a sub-group that will exhibit a particularly good response to anti-Hedgehog therapy.

KEY WORDS

Hedgehog, prostate cancer, reactive stroma, myofibroblast, paracrine, tumor microenvironment

INTRODUCTION

The Hedgehog (Hh) signaling pathway plays a pivotal role in the stromal-epithelial interactions of visceral organ development. The secreted ligand Sonic Hedgehog (Shh) activates an intracellular transduction mechanism in the target cell by binding to the plasma membrane

receptor Patched (Ptc). Ptc binding relieves inhibition of another membrane protein, Smoothened (Smo), and results in the activation of target gene transcription by members of the Gli transcription factor family. Gli1 or Gli2 proteins act as transcriptional activators. Both Ptc and Gli1 are transcriptional readouts of Gli1 and Gli2 activity and increased transcription of Gli1 and Ptc in the target cell serves as an indicator of Hh pathway activity. Gli3 behaves primarily as a repressor of Hh target gene expression in the absence of Shh; this inhibitory action is relieved by binding of ligand and activation of the Hh pathway. While the premier role of Hh signaling is in the developing embryo, the Hh pathway can be re-activated in adult tissues as part of the regenerative response to injury and sustained activation has been linked to tumor initiation and progression(Kelleher *et al.*, 2006). It is estimated that 25% of cancer deaths are associated with altered Hh signaling(Lum and Beachy, 2004) and evidence from several studies suggests that Hh pathway activity in prostate cancer promotes tumor growth, invasion, metastasis and hormone independence(Fan *et al.*, 2004; Karhadkar *et al.*, 2004; Sheng *et al.*, 2004).

The Hh pathway has been touted as a promising target for directed chemotherapy and Smo, Gli1 and Gli2 have been considered primary targets for anti-Hh therapeutics(Lauth and Toftgard, 2007b). A corn lily steroidal alkaloid, cyclopamine, inhibits intracellular Hh signaling by blocking the activity of Smo and has been used as a first generation Hh inhibitor in the treatment of localized basal cell carcinoma. Second generation Hh inhibitors mimic the action of cyclopamine or directly block the activity of Gli transcription factors(Lauth *et al.*, 2007). Efforts to develop and apply anti-Hh therapeutics have been underway for several years. Progress in the pre-clinical testing of these agents against prostate cancer will depend on understanding of the

important molecular mechanisms of Hh signaling in prostate cancer and the development and validation of an appropriate tumor model system.

The mechanism of Hh signaling in prostate cancer has been controversial. Surveys of Hh signaling in human prostate specimens revealed the presence of robust Hh signaling in both benign and malignant prostate tissue, with the finding of increased Hh signaling in advanced, metastatic disease. Tumor cell Shh expression was shown to promote the growth of human prostate cancer xenografts in mice and this was associated with increased expression of Gli1 within mouse stromal cells – suggesting a paracrine mechanism of effect(Fan *et al.*, 2004). Subsequent studies appeared to show the presence of autocrine signaling in human prostate cancer tissues. These studies showed that cyclopamine decreased growth of prostate cancer cells in vitro, in apparent support of an autocrine mechanism(Karhadkar *et al.*, 2004; Sanchez *et al.*, 2004), but it was later shown that the inhibition of prostate cancer cell proliferation is not accompanied by the expected changes in expression of the endogenous target genes Gli1 and Ptc(Levitt *et al.*, 2007; Zhang *et al.*, 2007). Further, it was shown that these prostate cancer cell lines do not respond to Shh ligand stimulation(Levitt *et al.*, 2007; McCarthy and Brown, 2008; Zhang *et al.*, 2007). This is not to say that autocrine signaling does not occur in prostate cancer. There is evidence for mutational activation of the Hh pathway in a ligand independent fashion and prostate cancer cells have been shown to respond to Gli inhibitors with decreased proliferation and transcription of Gli1 and Ptc(Lauth *et al.*, 2007). Taken together, the published evidence suggests that Hh signaling in prostate cancer may embrace both autocrine and paracrine mechanisms.

The studies presented here were designed to rigorously examine the mechanism of Hh signaling on growth of the LNCaP xenograft tumor and to then extend those observations to elucidate the contribution of paracrine Hh signaling in human prostate cancer. They support the conclusion that activation of the Hh pathway in tumor stromal cells, achieved by either ligand-dependent paracrine signaling or ligand-independent pathway activation, is sufficient to promote tumor growth. Hh pathway activation in the tumor stroma induces expression of genes identified as Hh-regulated genes in the fetal prostate. Nine target genes, induced by Shh in the developing prostate and by Shh over-expression in the LNCaP xenograft, comprise a signature of paracrine Hh signaling that is associated with growth stimulation. In human prostate tissue, a partial recapitulation of this Hh-regulated gene expression signature is associated with cancer and the complete signature is associated specifically with tumors exhibiting a reactive stroma.

MATERIALS AND METHODS

Xenografts

Xenograft tumors were generated in adult male CD-1 nude mice. $2x10^6$ LNCaP, LN-GFP or LN-Shh were mixed with $0.5x10^6$ INK4 cells and 50% Matrigel and injected subcutaneously on the flanks of mice. For 1:1 mix tumors, $1x10^6$ LNCaP and $1x10^6$ LN-Shh were combined and injected subcutaneously as described above. LN-GFP and LN-Shh stably express GFP or GFP+Shh, respectively(Fan *et al.*, 2004). Tumors were measured weekly with calipers and tumor volume was calculated as the volume of a spheroid using the formula: Vol = LxWxHx0.5236(Janik *et al.*, 1975).

Immunohistochemistry

Formalin-fixed paraffin embedded sections were dewaxed, rehydrated and processed for antigen retrieval 10 minutes in citrate buffer. GFP was stained by incubation with anti-GFP (Chemicon AB3080, Temecula, CA) diluted to 4 ug/ml in PBC + 10% (goat or donkey) serum + 1% BSA overnight at 4°C. Human Ki67 was stained by incubation with prediluted Ki67 antibody (Invitrogen catalog, Carlsbad, CA) for 1 hour at room temperature. Smooth muscle actin was stained by incubation with 1:200 anti-smooth muscle actin ascites (Sigma-Aldrich A2457, St. Louis, MO). In human sections, vimentin was stained by incubation with 1:100 anti-vimentin (Chemicon AB1620). In mouse sections, vimentin was stained by incubation with 1:100 anti-vimentin (Santa Cruz sc-7557). The primary antibodies were detected by incubation with goat or donkey anti-goat, anti-rabbit, or anti-mouse conjugated with Alexa 488 or Alexa 555 (Molecular Probes, Eugene, OR) at 5 ug/ml for 45 minutes at room temperature. Slides were mounted with Vectashield Hardset + DAPI mounting media (Vector, Burlingame, CA) and imaged using an Olympus model BX51 fluorescent microscope and Spot Advanced software v. 3.5.2. In xenografts, GFP and Ki67 and total tumor cells were counted in ten random 200x fields of view. Ki67 staining is human-specific, so proliferation of mouse stromal cells is not included. In patient tissues, Ki67, smooth muscle actin and vimentin were counted in five random 200x fields of view. For each sample, the frequency of myofibroblasts was determined by rating myofibroblasts/total stromal cells on the following scale: 1 = no myofibroblasts, 2 = 1-5% myofibroblasts, 3 = 5-25% myofibroblasts, 4 = >25% myofibroblasts. The frequency of myofibroblasts was determined for each of 5 random fields of view and totaled for each section to give scores that vary between 5-20. Samples with a score of 4-9 were ranked as non-reactive and samples with scores 10-20 are ranked as reactive. Analysis was performed in a blinded fashion so the analyst did not know of the benign, tumor, reactive, or gene expression nature of

the samples. The ranking of samples as reactive vs. non-reactive was determined before quantitative or correlation analysis of gene expression was performed.

Isolation of UGSM cells

Generation of UGSM-2 cells was described in a previous paper(Shaw *et al.*, 2006). To generate INK4a-/-, Gli3xt/xt mice, INK4a-/- mice were bred to Gli3xt/+ mice and then backcrossed to INK4a-/- mice to generate INK4a-/-, Gli3xt/+ mice. INK4a-/-, Gli3xt/+ mice were mated and embryos collected at embryonic day 16 (E16). The day of vaginal plug was counted as E0. Resulting embryos from a single litter included INK4a-/-, Gli3+/+; INK4a-/-, Gli3xt/+; and INK4a-/-, Gli3xt/xt. Urogenital sinus mesenchyme (UGSM) from male embryos was collected and cultured in the same manner as UGSM-2 cells. Embryo tissue was used for genotyping according to established protocols(Hui and Joyner, 1993). Clonal populations were isolated by ring cloning from the mixed primary cell population.

Gene expression analysis

RNA was isolated from cultured cells and tumors using RNeasy mini kit (Qiagen, Valencia, CA) with optional on-column DNase digestion to eliminate contaminating DNA. 1 ug of total RNA was reverse transcribed to generate cDNA using M-MLV reverse transcriptase (Invitrogen). Relative mRNA quantity was determined by real-time RT-PCR using iCycler instrumentation and software (BioRad, Hercules, CA).

Human prostate samples

Paired prostate cancer/ benign prostate tissue specimens were provided by the Tissue and Serum

Repository (Kansas Cancer Institute, University of Kansas Medical Center, Kansas City, KS). After removal of the prostate from men undergoing radical prostatectomy for clinically localized prostate cancer, core biopsies were performed of presumed tumor and the equivalent site on the contra-lateral side of the specimen. Each sample was divided and snap frozen or formalin fixed/paraffin embedded. Of the 44 specimens processed in this way, tumor and benign tissue from the same patient were confirmed by histologic examination. Some samples from the same patient are both benign or both tumor. The samples include 18 tumors and 26 benign tissues. 13 sets of these are matched. The institutional review boards of the University of Wisconsin-Madison and Kansas University Medical Center approved all procedures for tissue acquisition and analysis.

Statistics

We analyzed tumor growth rate by obtaining slopes. These were obtained by calculating the difference between final and initial tumor volumes, and then dividing by the intervening number of weeks: $(V_n - V_0)/n$, where V_0 denotes the tumor volume (in mm^3) when it first becomes apparent, V_n denotes the tumor volume n weeks later, and n is the number of weeks between tumor appearance and the end of the experiment or the week in which the animal needed to be euthanized, whichever occurred earlier. Tumors with one or more of the following conditions were excluded from the analysis: those with a final volume of less than $100mm^3$, those that contracted (i.e. final volume < initial volume), those that were undetectable in any given week post initial establishment, and those with a slope less than $10mm^3$/week. One-Way Analysis of Variance (ANOVA) was used to test for differences in growth rate (slope) due to treatment; slopes within a given animal were considered independent. If the overall *F*-test was significant

($P < 0.05$) pair-wise comparisons between treatments were examined. This procedure is equivalent to Fisher's protected least-squares differences (LSD). In order to better meet the assumptions of ANOVA, rank and logarithmic transformations of the original data were considered. Slopes for tumor growth seemed to have a slightly positive skew distribution. A logarithmic transformation did not improve matters, so ANOVA was performed on the raw slopes. We analyzed differences in gene expression by comparing the average GAPDH normalized value for each gene using a *t*-test assuming unequal variances. To examine the degree of linear association in expression between pairs of genes, Pearson's correlation coefficient was obtained. This was done (A) for all of the samples together (B) for the tumor and the benign samples separately; and (C) for each of the four tumor-reactivity groups (benign/tumor vs. reactive/non-reactive) separately. One-way analysis of variance (ANOVA) was used to test for differences in gene expression between the four tumor-reactivity groups. If significant differences were found, pair-wise comparisons were obtained (Fisher's protected LSD). In order to better meet the assumptions of ANOVA, the natural logarithms of expressions were analyzed, after having added 1E-4. $P < 0.05$ was used as the criterion for statistical significance; all hypothesis tests were two-sided. There was no adjustment for multiple testing. Both the correlation analysis and ANOVA treated the observations as independent. All the statistical graphics and computations were obtained in R for Windows, version 2.5.0 patched (2007-02-04 r40647) (R Development Core Team, 2005).

RESULTS

Autocrine Shh signaling does not regulate tumor growth

Gli2 is the linchpin of the transcriptional response to Hh ligand. This has been demonstrated in genetic studies(Bai *et al.,* 2002) and in cell-based assays where deletion of the Gli2 gene was found to reduce Shh-induced target gene expression by 50-70%(Lipinski *et al.,* 2006). The human prostate cancer cell line LNCaP does not respond to Shh ligand or transfection with oncogenic Smo, but transfection of LNCaP cells with Gli2 induces expression of both Ptc and Gli1(Zhang *et al.,* 2007). These studies point to a disruption in the canonical signal transduction mechanism upstream of Gli2 that precludes ligand-dependent pathway activation in LNCaP cells, but leaves open the possibility of a response to Hh ligand that is not associated with Gli1 and Ptc transcription or an alternative mechanism of Hh pathway activation mediated by selective changes in the activity of Gli2. Notably, it has been reported that Gli2 protein is increased in prostate cancer cells than in normal prostate epithelium, even though Gli2 mRNA is no more abundant(Bhatia *et al.*, 2006). To examine these possibilities, we tested the effect of blocking the Hh pathway with a dominant negative form of Gli2. The Gli2 mutB construct was cloned from a family with clinical features of Gli2 loss-of-function. MutB lacks the part of the C-terminal transactivation domain and acts to prevent Hh target gene activation by Gli2(Roessler *et al.*, 2005). We first showed that induction of Gli1 and Ptc expression by transient transfection of LNCaP with Gli2 was abrogated by co-transfection with mutB (Figure 1a). We stably transfected LNShh cells with mutB and achieved high expression without any effect on Shh, Ptc or Gli1 expression (Figure 1b) or proliferation in vitro (Figure 1c). LNShh and LNShh-mutB xenograft tumors exhibited the same increased growth rate as compared to LNCaP xenografts (Figure 1d).

Recent studies suggest the existence of a non-canonical pathway for Hh signaling that is not mediated by Smo or Gli proteins(Lauth and Toftgard, 2007a). To test whether the acceleration of tumor cell proliferation in LNShh xenografts involves non-canonical ligand-dependent effects, we examined tumor growth and cell proliferation in chimeric xenografts made by co-injecting equal numbers of parent LNCaP (GFP-) and LNShh (GFP+) cells. The chimeric and LNShh xenografts displayed the same accelerated rate of growth as compared to the parental LNCaP xenograft. GFP immunostaining revealed that the chimeric tumors were composed of a mixed population containing approximately equal numbers of LNCaP and LNShh cells (Figure 2a) and quantitative analysis of proliferation by Ki67 staining showed that LNCaP and LNShh cells proliferate at the same rate (Figure 2b). From these studies we conclude that LNCaP cell over-expression of Shh exerts a non-cell autonomous effect on proliferation.

A paracrine fingerprint

Using species-specific RT-PCR primers to examine gene expression in the human tumor cells and mouse stromal cells of LNCaP and LNShh xenograft tumors, we previously showed that expression of human Gli1 and Ptc was unchanged in LNShh tumors while mouse Gli1 and Ptc were both significantly increased(Fan *et al.*, 2004). These findings implied a paracrine mechanism of action in which mouse stromal cells respond to Shh secreted by LNShh tumor cells and exert reciprocal effects that promote tumor cell proliferation. The expression of several previously identified Shh target genes (Sfrp1, Cyclin D1, Bcl-2, FGF-10, BMP-4, FoxA1, VEGF and IGF-II) was not different in the stroma of LNCaP and LNShh tumors (data not shown). Hh target genes vary between tissues and we therefore developed a strategy to identify Hh-regulated stromal genes in the prostate. As a first step, we made bi-clonal xenografts by co-injecting

LNCaP cells with the immortalized urogenital sinus mesenchymal cell line UGSM-2(Shaw *et al.*, 2006). These tumors grow at the same rate as the canonical LNCaP xenograft; histologic examination revealed a stroma composed of both UGSM-2 cells and resident host stromal cells (data not shown). When LNShh cells were co-injected with UGSM-2, the bi-clonal xenografts grew at a faster rate than LNCaP+UGSM-2 xenografts, replicating the growth effect of Shh over-expression in the canonical xenografts (Figure 3a).

We then performed a microarray analysis of genes activated by Shh treatment of UGSM-2 cells as part of our studies of prostate development and validated 19 Shh regulated genes in the embryonic day 16 mouse urogenital sinus mesenchyme(Yu *et al.*, 2009). Expression of these 19 genes was examined in the stroma of LNCaP+UGSM2 and LNShh+UGSM2 bi-clonal xenograft tumors using species-specific RT-PCR. Nine genes exhibited significantly different expression in the LNShh xenograft stroma consistent with regulation by Shh (Figure 3b). The nine genes are: a disintegrin and metalloproteinase domain 12 (ADAM12), angiopoietin-4 (Agpt4), breast and kidney-expressed chemokine (BRAK) or CXCL14, fibrillin-2 (Fbn2), fibroblast growth factor-5 (Fgf5), hairy and enhancer of split 1 (Hes1), hydroxysteroid 11-beta dehydrogenase 1 (HSD11β1), insulin-like growth factor-6 (Igfbp6), and tissue inhibitor of metalloproteinase 3 (Timp3). Hh-regulated expression of these nine genes was postulated to be a “fingerprint” of tumor stroma in which paracrine signaling promotes tumor growth

Activated stromal Shh signaling is sufficient to accelerate tumor growth

To verify that activation of Hh target gene expression in tumor stromal cells is sufficient to accelerate tumor growth, we derived urogenital sinus mesenchymal cell lines from Gli3 mutant

mouse embryos. The Gli3xt is a spontaneous missense mutation that abrogates Gli3 activity(Schimmang *et al.*, 1993) and results in basal activation of the Hh pathway independent of Shh ligand(Lipinski *et al.*, 2006). We bred the Gli3xt mutation onto an INK4a mutant background. The INK4a mutation allows spontaneous immortalization of mesenchymal cells. We then harvested mesenchymal cells from the embryonic prostate of Gli3xt/xt or Gli3wt/wt littermates. Basal expression of Gli1 in Gli3xt/xt cells is elevated to a level comparable to the level of Gli1 expression induced by Shh in wildtype cells (Figure 4a). We then generated bi-clonal xenografts containing LNCaP cells and either Gli3xt/xt or Gli3wt/wt cells. Xenografts containing Gli3xt/xt cells grew significantly faster than xenografts containing Gli3wt/wt cells (Figure 4b). These observations demonstrate that urogenital sinus mesenchymal cells with constitutive activation of Hh target gene transcription accelerate tumor growth in the absence of Hh ligand.

Fingerprint in human tumors

Our previous quantitative analysis of Hh pathway activity revealed the unexpected finding of equivalent robust Shh and Gli1 expression in both localized prostate cancer and benign prostate tissue. This finding prompted us to speculate that the effect of paracrine Hh signaling on cell proliferation may depend on the stromal response to Hh ligand. Indeed, we have found in the developing prostate that Hh signaling promotes epithelial proliferation in the fetal prostate, but inhibits epithelial proliferation in the postnatal prostate (unpublished observations). When we compared expression of Shh, Gli1, Ptc and the nine genes of the fingerprint in specimens of clinically-derived prostate cancer (n=18) and benign prostate tissues (n=26), neither Shh nor Gli1 expression was significantly higher in cancer (Figure 5a), and of the nine target genes only

(BRAK) exhibited significantly increased expression in cancer, a finding previously reported(Schwarze *et al.*, 2005). We then performed correlation analysis to identify genes that share a common regulatory pathway or function(Gustin *et al.*, 2008; Stuart *et al.*, 2003) with Hh signaling. We examined the correlation of expression among Shh, Gli1, Gli2, Ptc and the nine genes of the stromal fingerprint in all specimens examined and compared these findings in subgroups of interest. Analysis of all tissues, regardless of histopathology, showed that the expression of Shh, Gli1, Gli2 and Igfbp6 was significantly correlated in all pair-wise combinations of these genes (Supplemental Figure 1). Analysis of Indian Hedgehog (Ihh) expression showed no correlation with Gli1 or Gli2, indicating that Gli1 and Gli2 expression relates to specifically to the expression of Shh. Correlation analysis was then performed separately as tissues were grouped as benign or cancer. For the benign samples, there was clustering of Shh, Gli1, Gli2, BRAK and Igfbp6 expression. For the cancer samples, there was clustering of Shh, Gli1, Gli2, Igfbp6, ADAM12, Agpt4, HSD11b1 and Timp3 (Figure 5b). Remarkably, the expression of these genes in cancer was significantly correlated in all pair-wise combinations and all genes were positively correlated (Supplemental Figure 2). The clustering of Shh, Gli1, Gli2 and IGFBP6 shows Shh-regulated gene expression is present in benign and cancerous tissue, but, the unique clustering of ADAM12, Agpt4, HSD11b1 and Timp3 with Shh and Gli1 in cancer suggests an altered stromal response to Shh in stroma associated with cancer versus benign epithelium.

Reactive stroma in prostate tissue

We wondered if further characterization of the tumor stroma would isolate the gene expression networks. Myofibroblasts are stromal cells that express both fibroblast (vimentin) and smooth

muscle markers (smooth muscle actin, SMA), exhibit a unique ultra-structure associated with extracellular matrix remodeling, and are found in developing tissues, granulation tissue, and neoplasia(Tuxhorn *et al.*, 2001). Myofibroblasts are found in both the developing mouse and human prostates(Bierhoff *et al.*, 1997); they are generally absent from the adult mouse prostate but are present to variable degrees in the adult human prostate. In the human prostate, myofibroblasts appear to be especially abundant in areas of malignant transformation, where their presence has been considered a hallmark of a reactive stroma(Tuxhorn *et al.*, 2001). Our studies revealed that myofibroblasts are a consistent feature of both LNCaP and LNShh xenograft tumors (Supplemental Figure 3). Since the UGSM-2 cell line that was used to identify stromal Hh target genes exhibits a myofibroblast phenotype, we examined the possibility that the nine gene fingerprint genes identified in the myofibroblastic xenografts is specific to reactive stroma. The same tissues analyzed by RT-PCR for the correlation studies described above were co-stained for smooth muscle actin and vimentin. Myofibroblasts, which stain for both smooth muscle actin and vimentin, were present in varying degrees in both benign and malignant tissue (Supplemental Figure 3). Immunostaining was scored in blinded fashion and the stroma was categorized as reactive or non-reactive based on the abundance of myofibroblasts. Thus the 44 tissue samples were divided into 4 groups: 9 tumor reactive, 9 tumor non-reactive, 15 benign reactive, and 11 benign non-reactive. The reactive score does not correlate with Gleason score or stromal density (Supplemental Figure 4). There were no significant differences in target gene expression between any of the 4 groups, except for BRAK as previously described (Supplemental Figure 5). Correlation analysis showed that Shh expression correlates with Gli1 and Gli2 in all four groups. The striking finding is the clustering of Shh, Gli1, Ptc and all 9 genes of the complete fingerprint uniquely in the tumor reactive samples (Figure 6a). Analysis

of proliferation in these tissues showed that proliferation is highest in the tumor reactive group (Figure 5c).

DISCUSSION

A recently published study revealed increased Hedgehog pathway activity in a variety of tumor types(Yauch *et al.*, 2008) and there is evidence that metastatic and androgen-independent prostate cancer exhibit markedly elevated pathway activity(Fan *et al.*, 2004; Karhadkar *et al.*, 2004). However, a meticulous comparison of Hh signaling in localized prostate cancer and benign control tissues did not demonstrate consistently increased pathway activity in cancer; rather, this study revealed robust Shh expression and Hh pathway activity in both benign and malignant tissues(Fan *et al.*, 2004). These findings were re-capitulated here with an entirely new set of cancer and benign specimens. Active signaling is present in both benign and cancer tissues, evidenced by the consistent correlation between Shh and Gli1 expression. The results presented here address and definitively answer several critical questions raised by these observations with respect to the action of Sonic Hedgehog in prostate cancer. First, we show that action of Shh on carcinoma cells (autocrine signaling) is not necessary for acceleration of tumor cell proliferation. Rather, secreted Shh induces a non-autonomous paracrine signaling network in tumor stroma that stimulates growth. Second, we show that Hh pathway activation in a myofibroblast component of the tumor stroma is sufficient to accelerate tumor growth. The accelerating effect of Gli3xt/xt myofibroblast cells on tumor growth signifies that the growth accelerating effect of Shh over-expression in the LNShh tumor does not depend on a direct effect of Shh ligand on other components of the stroma. This is critical since both endothelial cells and immune cells have been identified as targets of Hh signaling. Finally, we have identified a

transcriptional signature of Hh signaling in the LNShh xenograft, related to the transcriptional read-out of the fetal prostate mesenchyme, that is faithfully recapitulated specifically in human prostate cancers exhibiting a reactive stroma.

Insight into the mechanisms determining the stromal mediation of Hh signaling will be crucial to evaluating the utility and efficacy of Hh inhibitors in the treatment of prostate cancer. Karhadkar and colleagues demonstrated that Hh blockade by the Smo inhibitor cyclopamine could inhibit xenograft tumor growth(Karhadkar *et al.*, 2004) and recent studies suggest that the inhibition of growth results from blockade of paracrine Hh signaling(Yauch *et al.*, 2008). This is consistent with the studies presented here and our previous work identifying paracrine signaling as the primary Hh mechanism in localized prostate cancer(Fan *et al.*, 2004). Studies attempting to correlate a clinical response to Hh inhibitors with events at the cellular level will need to examine the effect of Hh blockade on pathway activity in the tumor stroma. The data reported here provide a gene expression signature that is a putative biomarker of growth-promotion and suggest that tumors with a reactive stroma, which exhibit this signature, are more likely to exhibit a favorable clinical response to Hh inhibitors.

Canonical Hh signaling involving the tumor stroma may not be the only Hh mechanism stimulating human prostate cancer progression. Indeed, there is evidence to suggest that non-canonical activation of autocrine Hh pathway activity may occur, especially in advanced prostate cancer. Hh pathway activity resulting from mutational activation in the Hh signal transduction mechanism or by aberrant pathway activation could be unresponsive to Smo inhibition and require alternate therapeutic approaches(Lauth and Toftgard, 2007b; Sheng *et al.*, 2004).

Notably, recent studies showed that Gli1 inhibitors GANT61 and GANT58 could be used to inhibit proliferation of tumor cells in which such Hh pathway activation has occurred(Lauth *et al.*, 2007).

Previous studies have highlighted the potential significance role of myofibroblasts in prostate cancer stroma. Rowley, Ayala and colleagues have shown that myofibroblasts stimulate growth of xenograft tumors and that the accumulation of myofibroblasts in human prostate cancer is negatively correlated with tumor-free survival(Tuxhorn *et al.*, 2002; Yanagisawa *et al.*, 2008). Whereas Shh-accelerated growth of LNShh xenografts was associated with increased expression of the nine Hh target genes, we did not observe increased expression of these target genes in human prostate cancer. Efforts to perform a meta-analysis of this gene network using the microarray data sets on the cancer profiling database Oncomine(Rhodes *et al.*, 2005; Rhodes *et al.*, 2007a; Rhodes *et al.*, 2007b; Rhodes *et al.*, 2004) was stymied by the absence of Gli1, Ptc and several of the target genes from the data sets. What we did observe from analysis of our own tissue set was a striking and statistically powerful correlation between expression of Shh and the tumor-fingerprint target genes, most strikingly in tumors with a reactive stroma. The best explanation for this finding is that emergence of a stromal phenotype in cancer that resembles the fetal mesenchyme results in a coordinate regulation of target genes that mimics the fetal transcriptional response to Shh. Since expression of these genes is not up regulated in cancer, it could be argued that an effect of Hh signaling on tumor growth is unlikely. Recognizing the validity of this argument, we postulate that the emergence of coordinate target gene regulation in the tumor stroma is a characteristic of a mesenchymal/stromal phenotype that responds to Hh ligand by exerting growth promoting activities that stimulate tumor cell proliferation.

ACKNOWLEDGEMENTS

We thank Alejandro Muñoz, Ph.D. and Glen Leverson, Ph.D. for assistance with statistical analysis. The Gli2-mutB expression construct was generously provided by Maximilian Muenke at NIH (Bethesda, MD). This work was supported by the Department of Defense Prostate Cancer Program Graduate Training Award W81XWH-06-1-0060 (Dr. Shaw), Department of Defense Award W81XWH-04-1-0263, and the NIDDK Award DK056238-06.

CONFLICT OF INTEREST

The authors declare no conflict of interest.

REFERENCES

Bai CB, Auerbach W, Lee JS, Stephen D, Joyner AL (2002). Gli2, but not Gli1, is required for initial Shh signaling and ectopic activation of the Shh pathway. *Development* 129: 4753-61.

Bhatia N, Thiyagarajan S, Elcheva I, Saleem M, Dlugosz A, Mukhtar H *et al* (2006). Gli2 is targeted for ubiquitination and degradation by beta-TrCP ubiquitin ligase. *J Biol Chem* 281: 19320-6.

Bierhoff E, Walljasper U, Hofmann D, Vogel J, Wernert N, Pfeifer U (1997). Morphological analogies of fetal prostate stroma and stromal nodules in BPH. *Prostate* 31: 234-40.

Fan L, Pepicelli CV, Dibble CC, Catbagan W, Zarycki JL, Laciak R *et al* (2004). Hedgehog signaling promotes prostate xenograft tumor growth. *Endocrinology* 145: 3961-70.

Gustin MP, Paultre CZ, Randon J, Bricca G, Cerutti C (2008). Functional meta-analysis of double connectivity in gene coexpression networks in mammals. *Physiol Genomics* 34: 34-41.

Hui CC, Joyner AL (1993). A mouse model of greig cephalopolysyndactyly syndrome: the extra-toesJ mutation contains an intragenic deletion of the Gli3 gene. *Nat Genet* 3: 241-6.

Janik P, Briand P, Hartmann NR (1975). The effect of estrone-progesterone treatment on cell proliferation kinetics of hormone-dependent GR mouse mammary tumors. *Cancer Res* 35: 3698-704.

Karhadkar SS, Bova GS, Abdallah N, Dhara S, Gardner D, Maitra A *et al* (2004). Hedgehog signalling in prostate regeneration, neoplasia and metastasis. *Nature* 431: 707-12.

Kelleher FC, Fennelly D, Rafferty M (2006). Common critical pathways in embryogenesis and cancer. *Acta Oncol* 45: 375-88.

Lauth M, Bergstrom A, Shimokawa T, Toftgard R (2007). Inhibition of GLI-mediated transcription and tumor cell growth by small-molecule antagonists. *Proc Natl Acad Sci U S A* 104: 8455-60.

Lauth M, Toftgard R (2007a). Non-canonical activation of GLI transcription factors: implications for targeted anti-cancer therapy. *Cell Cycle* 6: 2458-63.

Lauth M, Toftgard R (2007b). The Hedgehog pathway as a drug target in cancer therapy. *Curr Opin Investig Drugs* 8: 457-61.

Levitt RJ, Zhao Y, Blouin MJ, Pollak M (2007). The hedgehog pathway inhibitor cyclopamine increases levels of p27, and decreases both expression of IGF-II and activation of Akt in PC-3 prostate cancer cells. *Cancer Lett*.

Lipinski RJ, Gipp JJ, Zhang J, Doles JD, Bushman W (2006). Unique and complimentary activities of the Gli transcription factors in Hedgehog signaling. *Exp Cell Res* 312: 1925-38.

Lum L, Beachy PA (2004). The Hedgehog response network: sensors, switches, and routers. *Science* 304: 1755-9.

McCarthy FR, Brown AJ (2008). Autonomous Hedgehog signalling is undetectable in PC-3 prostate cancer cells. *Biochem Biophys Res Commun* 373: 109-12.

Rhodes DR, Kalyana-Sundaram S, Mahavisno V, Barrette TR, Ghosh D, Chinnaiyan AM (2005). Mining for regulatory programs in the cancer transcriptome. *Nat Genet* 37: 579-83.

Rhodes DR, Kalyana-Sundaram S, Mahavisno V, Varambally R, Yu J, Briggs BB *et al* (2007a). Oncomine 3.0: genes, pathways, and networks in a collection of 18,000 cancer gene expression profiles. *Neoplasia* 9: 166-80.

Rhodes DR, Kalyana-Sundaram S, Tomlins SA, Mahavisno V, Kasper N, Varambally R *et al* (2007b). Molecular concepts analysis links tumors, pathways, mechanisms, and drugs. *Neoplasia* 9: 443-54.

Rhodes DR, Yu J, Shanker K, Deshpande N, Varambally R, Ghosh D *et al* (2004). ONCOMINE: a cancer microarray database and integrated data-mining platform. *Neoplasia* 6: 1-6.

Roessler E, Ermilov AN, Grange DK, Wang A, Grachtchouk M, Dlugosz AA *et al* (2005). A previously unidentified amino-terminal domain regulates transcriptional activity of wild-type and disease-associated human GLI2. *Hum Mol Genet* 14: 2181-8.

Sanchez P, Hernandez AM, Stecca B, Kahler AJ, DeGueme AM, Barrett A *et al* (2004). Inhibition of prostate cancer proliferation by interference with SONIC HEDGEHOG-GLI1 signaling. *Proc Natl Acad Sci U S A* 101: 12561-6.

Schimmang T, van der Hoeven F, Ruther U (1993). Gli3 expression is affected in the morphogenetic mouse mutants add and Xt. *Prog Clin Biol Res* 383A: 153-61.

Schwarze SR, Luo J, Isaacs WB, Jarrard DF (2005). Modulation of CXCL14 (BRAK) expression in prostate cancer. *Prostate* 64: 67-74.

Shaw A, Papadopoulos J, Johnson C, Bushman W (2006). Isolation and characterization of an immortalized mouse urogenital sinus mesenchyme cell line. *Prostate* 66: 1347-58.

Sheng T, Li C, Zhang X, Chi S, He N, Chen K *et al* (2004). Activation of the hedgehog pathway in advanced prostate cancer. *Mol Cancer* 3: 29.

Stuart JM, Segal E, Koller D, Kim SK (2003). A gene-coexpression network for global discovery of conserved genetic modules. *Science* 302: 249-55.

Tuxhorn JA, Ayala GE, Rowley DR (2001). Reactive stroma in prostate cancer progression. *J Urol* 166: 2472-83.

Tuxhorn JA, Ayala GE, Smith MJ, Smith VC, Dang TD, Rowley DR (2002). Reactive stroma in human prostate cancer: induction of myofibroblast phenotype and extracellular matrix remodeling. *Clin Cancer Res* 8: 2912-23.

Yanagisawa N, Li R, Rowley D, Liu H, Kadmon D, Miles BJ *et al* (2008). Reprint of: Stromogenic prostatic carcinoma pattern (carcinomas with reactive stromal grade 3) in needle biopsies predicts biochemical recurrence-free survival in patients after radical prostatectomy. *Hum Pathol* 39: 282-91.

Yauch RL, Gould SE, Scales SJ, Tang T, Tian H, Ahn CP *et al* (2008). A paracrine requirement for hedgehog signalling in cancer. *Nature* 455: 406-10.

Yu M, Gipp J, Yoon JW, Iannaccone P, Walterhouse D, Bushman W (2009). Sonic hedgehog-responsive genes in the fetal prostate. *J Biol Chem* 284: 5620-9.

Zhang J, Lipinski R, Shaw A, Gipp J, Bushman W (2007). Lack of demonstrable autocrine hedgehog signaling in human prostate cancer cell lines. *J Urol* 177: 1179-85.

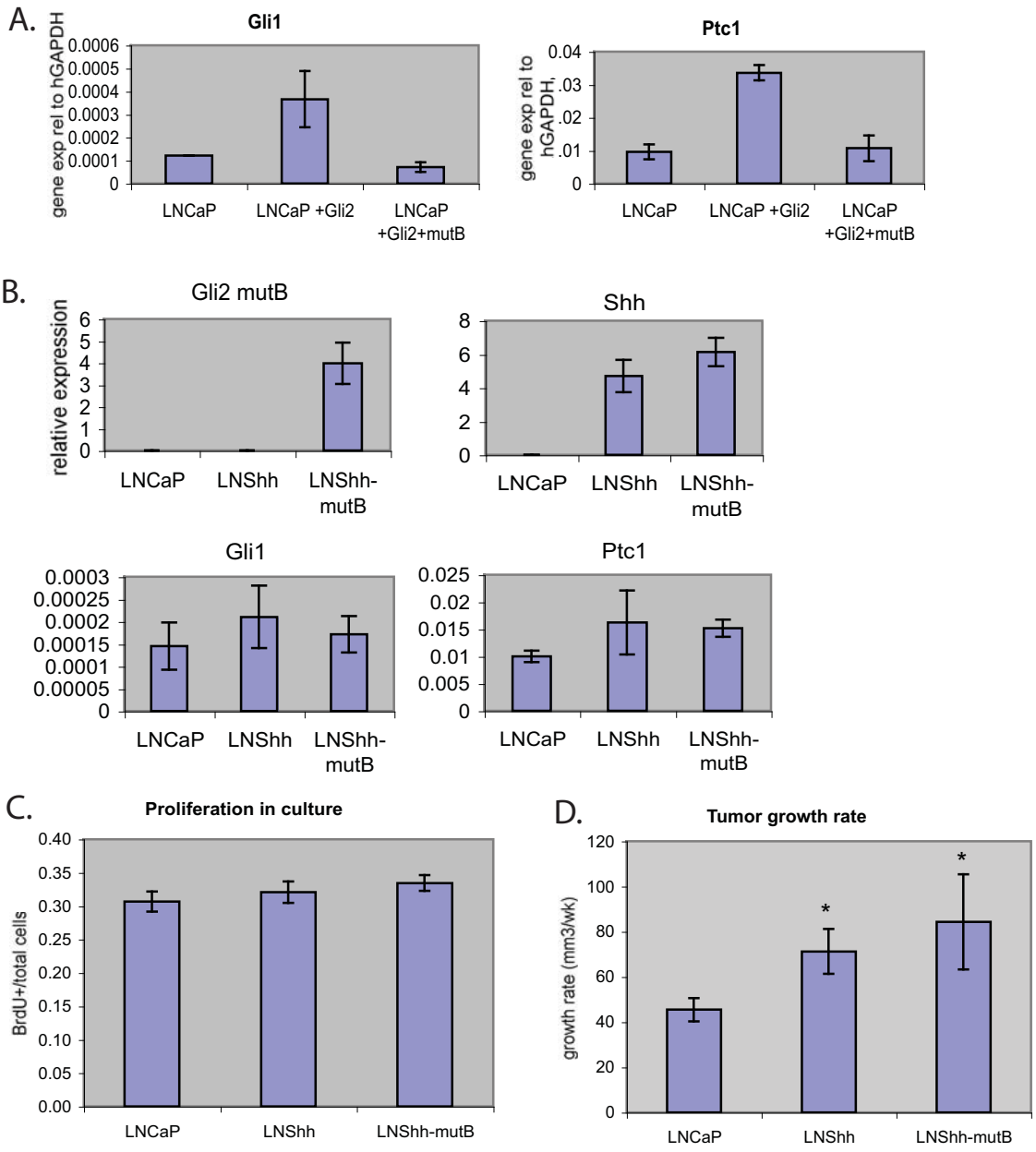

Figure 1. Dominant negative Gli2 (mutB) over-expression in LNCaP. (A) Transient expression of Gli2 or mutB in LNCaP for 48 hours reveals that mutB blocks Gli1 and Ptc1 induction by Gli2. (B) Stable expression of mutB in LNShh cells does not reduce Gli1 or Ptc1 expression. LNCaP-mutB cells do not proliferate/survive in culture. (C-left) MutB expression does not alter cell proliferation in culture. (D) MutB expression does not alter growth rate of tumors. Shh accelerates growth of tumors independent of mutB expression. *$p<0.05$ for comparison to LNCaP tumor growth rates.

A.

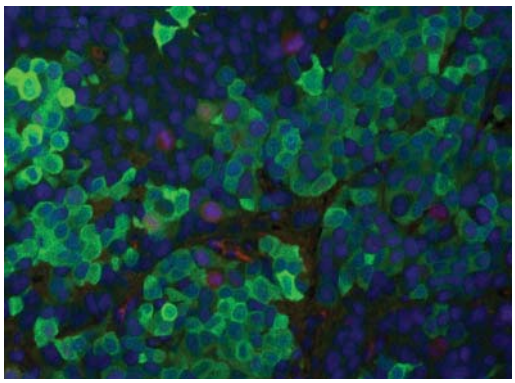

B.

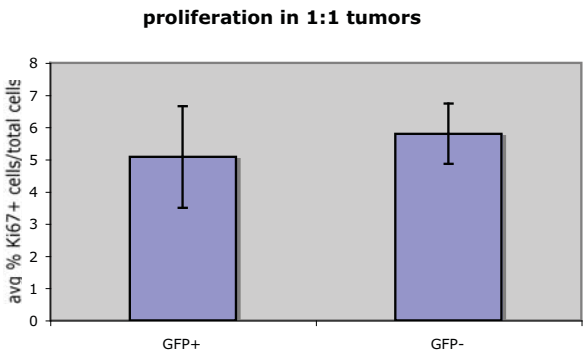

Figure 2. Shh does not cause cell autonomous tumor growth. (A) 1:1 mix tumors co-immunostained with GFP (green) + Ki67 (red) + DAPI (blue). Tumors are composed of 64% (+/- 4%) GFP+ LNShh cells (data not shown). (B) Proliferation rates are equivalent in LNShh (GFP+) and LNCaP (GFP-) cells in the same tumor.

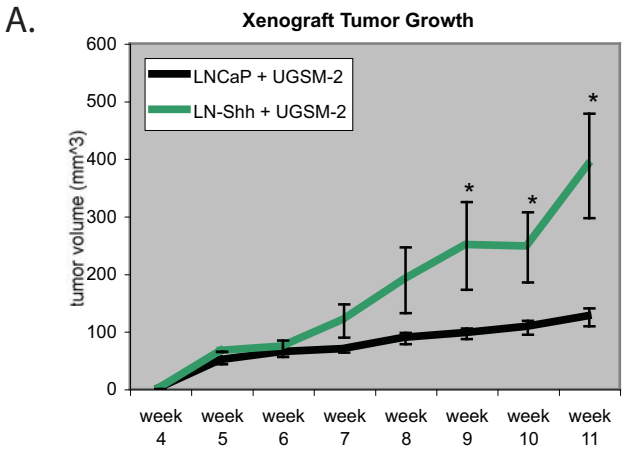

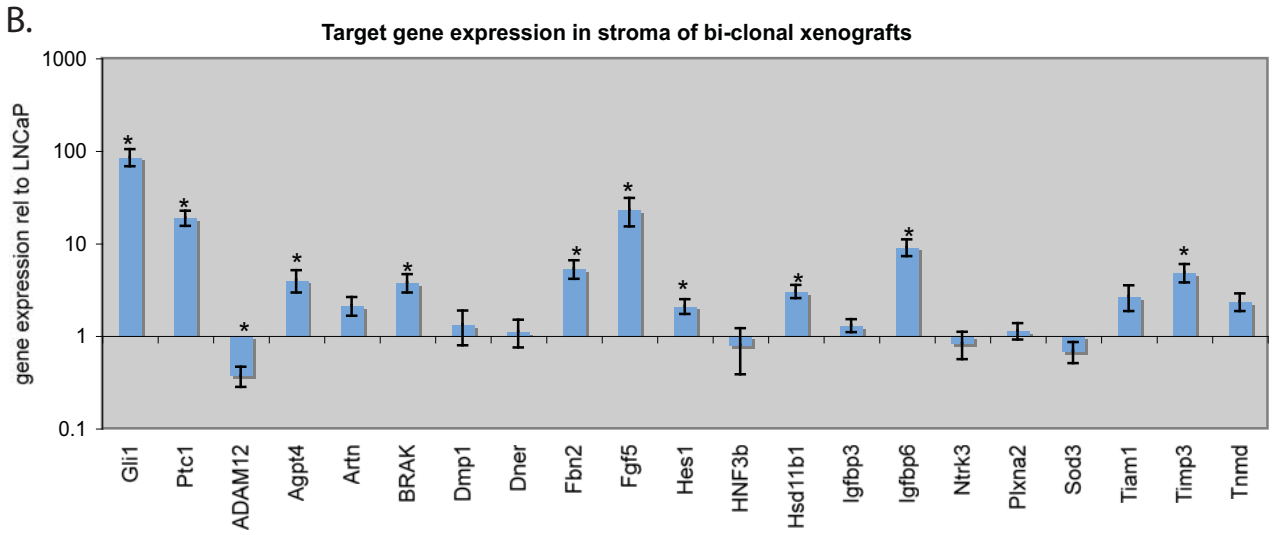

Figure 3. Bi-clonal xenograft tumors. (A) Shh accelerates tumor growth in bi-clonal xenografts composed of LNShh + UGSM2 stromal cells over that of LNCaP + UGSM2 xenografts. * indicates a significant ($P<0.05$) difference between tumor sizes at the week indicated. (B) Species-specific RT-PCR was used to analyze expression of Shh target genes in mouse stromal cells of bi-clonal xenografts. The chart shows the ratio of expression of target genes in LNShh xenografts relative to LNCaP xenografts. * $p<0.05$

A.

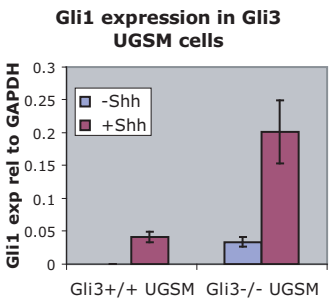

B.

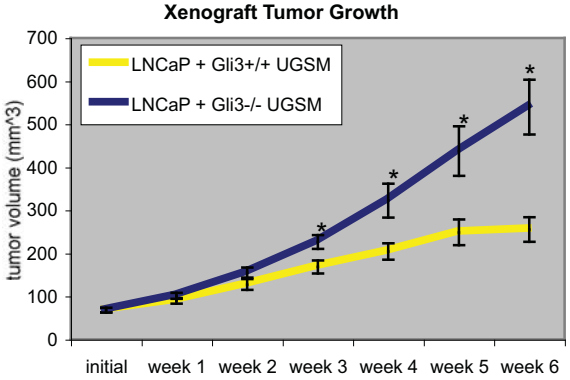

Figure 4. Stromal cells with increased Gli1 induce tumor growth independent of Shh. (A) RT-PCR analysis of Gli1 in Gli3+/+ and Gli3-/- UGSM cells that were treated with 10nM Shh. Values were normalized to the housekeeping gene GAPDH. (B) Weekly growth of LNCaP + Gli3+/+ and LNCaP + Gli3-/- bi-clonal xenografts. *significantly different from Gli3+/+ at the week indicated, $p<0.05$.

A.

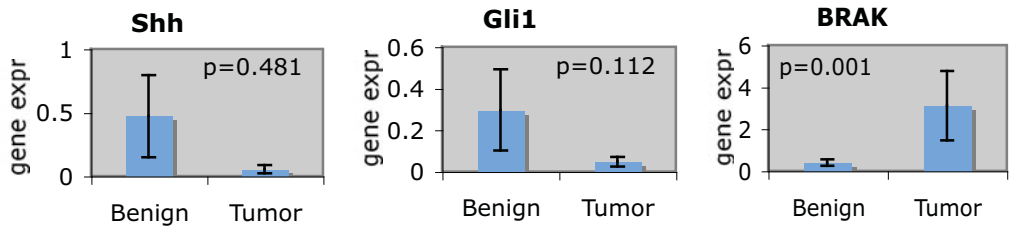

B.

tumor samples only

n=18	Shh	Gli1	Gli2	Ptc1	Hip	ADAM12	Agpt4	BRAK	Fbn2	Fgf5	Hes1	HSD11b1	Igfbp6	Timp3
Shh		0.0000	0.0000	0.8095	0.2022	0.0000	0.0000	0.8726	0.5810	0.4435	0.6199	0.0006	0.0000	0.0000
Gli1	0.0000		0.0000	0.6221	0.1567	0.0000	0.0000	0.6805	0.6490	0.5218	0.4796	0.0002	0.0000	0.0000
Gli2	0.0000	0.0000		0.1986	0.0363	0.0000	0.0000	0.2857	0.8439	0.7321	0.1971	0.0000	0.0000	0.0000
Ptc1	0.8095	0.6221	0.1986		0.0002	0.2181	0.4340	0.0000	0.2438	0.2460	0.0034	0.0099	0.4800	0.1294
Hip	0.2022	0.1567	0.0363	0.0002		0.0217	0.1766	0.1009	0.4560	0.9298	0.1724	0.0295	0.1373	0.0325
ADAM12	0.0000	0.0000	0.0000	0.2181	0.0217		0.0000	0.3296	0.7831	0.5063	0.2875	0.0000	0.0000	0.0000
Agpt4	0.0000	0.0000	0.0000	0.4340	0.1766	0.0000		0.3894	0.6103	0.6915	0.3666	0.0000	0.0000	0.0000
BRAK	0.8726	0.6805	0.2857	0.0000	0.1009	0.3296	0.3894		0.3075	0.2478	0.0000	0.0030	0.4797	0.1946
Fbn2	0.5810	0.6490	0.8439	0.2438	0.4560	0.7831	0.6103	0.3075		0.5518	0.0173	0.9638	0.8424	0.8595
Fgf5	0.4435	0.5218	0.7321	0.2460	0.9298	0.5063	0.6915	0.2478	0.5518		0.2628	0.9503	0.7392	0.9962
Hes1	0.6199	0.4796	0.1971	0.0034	0.1724	0.2875	0.3666	0.0000	0.0173	0.2628		0.0180	0.2678	0.1019
HSD11b1	0.0006	0.0002	0.0000	0.0099	0.0295	0.0000	0.0000	0.0030	0.9638	0.9503	0.0180		0.0000	0.0000
Igfbp6	0.0000	0.0000	0.0000	0.4800	0.1373	0.0000	0.0000	0.4797	0.8424	0.7392	0.2678	0.0000		0.0000
Timp3	0.0000	0.0000	0.0000	0.1294	0.0325	0.0000	0.0000	0.1946	0.8595	0.9962	0.1019	0.0000	0.0000	

benign samples only

n=26	Shh	Gli1	Gli2	Ptc1	Hip	ADAM12	Agpt4	BRAK	Fbn2	Fgf5	Hes1	HSD11b1	Igfbp6	Timp3
Shh		0.0000	0.0000	0.4873	0.4994	0.9126	0.7893	0.0000	0.3622	0.2616	0.6296	0.3050	0.0022	0.2267
Gli1	0.0000		0.0000	0.5171	0.3911	0.8395	0.6543	0.0000	0.4334	0.2933	0.6059	0.3217	0.0053	0.2280
Gli2	0.0000	0.0000		0.6608	0.0034	0.1607	0.1314	0.0000	0.1109	0.7655	0.4641	0.6936	0.0000	0.0002
Ptc1	0.4873	0.5171	0.6608		0.0046	0.7210	0.8438	0.6831	0.0061	0.0000	0.0553	0.3924	0.7079	0.0216
Hip	0.4994	0.3911	0.0034	0.0046		0.9265	0.0006	0.6613	0.0000	0.0909	0.0992	0.9787	0.2496	0.0067
ADAM12	0.9126	0.8395	0.1607	0.7210	0.9265		0.3815	0.3512	0.8220	0.9169	0.0431	0.8536	0.0000	0.0831
Agpt4	0.7893	0.6543	0.1314	0.8438	0.0006	0.3815		0.6216	0.2067	0.7780	0.7839	0.4815	0.6034	0.3373
BRAK	0.0000	0.0000	0.0000	0.6831	0.6613	0.3512	0.6216		0.5148	0.4409	0.8502	0.3740	0.0001	0.0997
Fbn2	0.3622	0.4334	0.1109	0.0061	0.0000	0.8220	0.2067	0.5148		0.0589	0.0042	0.2087	0.5992	0.0035
Fgf5	0.2616	0.2933	0.7655	0.0000	0.0909	0.9169	0.7780	0.4409	0.0589		0.0279	0.0324	0.9060	0.1024
Hes1	0.6296	0.6059	0.4641	0.0553	0.0992	0.0431	0.7839	0.8502	0.0042	0.0279		0.2924	0.0773	0.0073
HSD11b1	0.3050	0.3217	0.6936	0.3924	0.9787	0.8536	0.4815	0.3740	0.2087	0.0324	0.2924		0.7210	0.1920
Igfbp6	0.0022	0.0053	0.0000	0.7079	0.2496	0.0000	0.6034	0.0001	0.5992	0.9060	0.0773	0.7210		0.0031
Timp3	0.2267	0.2280	0.0002	0.0216	0.0067	0.0831	0.3373	0.0997	0.0035	0.1024	0.0073	0.1920	0.0031	

C.

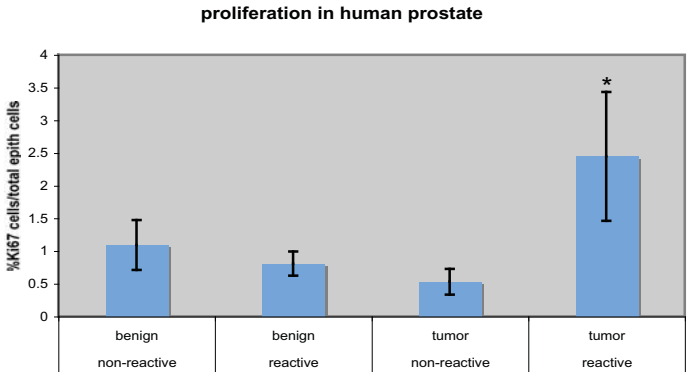

Figure 5. Analysis of Shh paracrine target genes in human prostate benign and tumor tissue. (A) Expression of Shh, Gli1 is equal when comparing benign and tumor tissue from the same prostate. Expression of BRAK is the only gene whose expression varies when comparing benign and tumor tissue from the same prostate. Expression of the other target genes does not vary. (B) Co-expression of hedgehog signaling and target genes was analyzed by Pearson product-moment correlation. The numbers listed are correlation p-values. Values less than 0.05 are highlighted. Each of the highlighted correlations is a positive correlation. (C) Proliferation of human prostate tissue assayed by Ki67 immunohistochemistry. *p<0.05

tumor reactive

n=9	Shh	Gli1	Gli2	Ptc1	Hip	ADAM12	Agpt4	BRAK	Fbn2	Fgf5	Hes1	HSD11b1	Igfbp6	Timp3
Shh		0.0054	0.0038	0.0031	0.0036	0.0129	0.0062	0.0153	0.0124	0.2271	0.0543	0.0049	0.0583	0.0439
Gli1	0.0054		0.0000	0.0000	0.0003	0.0036	0.0006	0.0000	0.0059	0.0188	0.0044	0.0000	0.0012	0.0002
Gli2	0.0038	0.0000		0.0000	0.0012	0.0047	0.0021	0.0000	0.0015	0.0119	0.0007	0.0002	0.0006	0.0001
Ptc1	0.0031	0.0000	0.0000		0.0002	0.0012	0.0009	0.0003	0.0008	0.0175	0.0056	0.0002	0.0016	0.0002
Hip	0.0036	0.0003	0.0012	0.0002		0.0000	0.0072	0.0096	0.0020	0.0757	0.0390	0.0006	0.0094	0.0052
ADAM12	0.0129	0.0036	0.0047	0.0012	0.0000		0.0360	0.0244	0.0007	0.0446	0.0524	0.0096	0.0079	0.0059
Agpt4	0.0062	0.0006	0.0021	0.0009	0.0072	0.0360		0.0021	0.0442	0.1691	0.0566	0.0001	0.0505	0.0172
BRAK	0.0153	0.0000	0.0000	0.0003	0.0096	0.0244	0.0021		0.0236	0.0078	0.0004	0.0003	0.0005	0.0001
Fbn2	0.0124	0.0059	0.0015	0.0008	0.0020	0.0007	0.0442	0.0236		0.0272	0.0186	0.0232	0.0080	0.0053
Fgf5	0.2271	0.0188	0.0119	0.0175	0.0757	0.0446	0.1691	0.0078	0.0272		0.0016	0.0693	0.0001	0.0003
Hes1	0.0543	0.0044	0.0007	0.0056	0.0390	0.0524	0.0566	0.0004	0.0186	0.0016		0.0137	0.0001	0.0004
HSD11b1	0.0049	0.0000	0.0002	0.0002	0.0006	0.0096	0.0001	0.0003	0.0232	0.0693	0.0137		0.0076	0.0027
Igfbp6	0.0583	0.0012	0.0006	0.0016	0.0094	0.0079	0.0505	0.0005	0.0080	0.0001	0.0001	0.0076		0.0000
Timp3	0.0439	0.0002	0.0001	0.0002	0.0052	0.0059	0.0172	0.0001	0.0053	0.0003	0.0004	0.0027	0.0000	

tumor non-reactive

n=9	Shh	Gli1	Gli2	Ptc1	Hip	ADAM12	Agpt4	BRAK	Fbn2	Fgf5	Hes1	HSD11b1	Igfbp6	Timp3
Shh		0.0000	0.0000	0.9138	0.4108	0.0001	0.0000	0.4769	0.5704	0.4265	0.5483	0.0000	0.0000	0.0000
Gli1	0.0000		0.0000	0.8677	0.4067	0.0002	0.0000	0.4477	0.5931	0.4265	0.5367	0.0000	0.0000	0.0000
Gli2	0.0000	0.0000		0.6664	0.2647	0.0001	0.0000	0.4586	0.6477	0.4485	0.5378	0.0000	0.0000	0.0000
Ptc1	0.9138	0.8677	0.6664		0.0111	0.8783	0.9839	0.8027	0.5550	0.9968	0.8241	0.8543	0.8613	0.5729
Hip	0.4108	0.4067	0.2647	0.0111		0.2693	0.5359	0.8063	0.9271	0.5099	0.9721	0.5034	0.4281	0.2734
ADAM12	0.0001	0.0002	0.0001	0.8783	0.2693		0.0007	0.6241	0.5628	0.2776	0.6645	0.0005	0.0003	0.0009
Agpt4	0.0000	0.0000	0.0000	0.9839	0.5359	0.0007		0.4551	0.5448	0.5351	0.5707	0.0000	0.0000	0.0000
BRAK	0.4769	0.4477	0.4586	0.8027	0.8063	0.6241	0.4551		0.0082	0.8237	0.0000	0.3718	0.3715	0.3202
Fbn2	0.5704	0.5931	0.6477	0.5550	0.9271	0.5628	0.5448	0.0082		0.9332	0.0020	0.6240	0.6839	0.8192
Fgf5	0.4265	0.4265	0.4485	0.9968	0.5099	0.2776	0.5351	0.8237	0.9332		0.8139	0.4781	0.4727	0.5054
Hes1	0.5483	0.5367	0.5378	0.8241	0.9721	0.6645	0.5707	0.0000	0.0020	0.8139		0.5223	0.4621	0.4035
HSD11b1	0.0000	0.0000	0.0000	0.8543	0.5034	0.0005	0.0000	0.3718	0.6240	0.4781	0.5223		0.0000	0.0000
Igfbp6	0.0000	0.0000	0.0000	0.8613	0.4281	0.0003	0.0000	0.3715	0.6839	0.4727	0.4621	0.0000		0.0000
Timp3	0.0000	0.0000	0.0000	0.5729	0.2734	0.0009	0.0000	0.3202	0.8192	0.5054	0.4035	0.0000	0.0000	

benign reactive

n=15	Shh	Gli1	Gli2	Ptc1	Hip	ADAM12	Agpt4	BRAK	Fbn2	Fgf5	Hes1	HSD11b1	Igfbp6	Timp3
Shh		0.0000	0.0002	0.4152	0.5587	0.9729	0.3807	0.0000	0.3023	0.2993	0.6328	0.2738	0.0285	0.4680
Gli1	0.0000		0.0003	0.4296	0.4950	0.8461	0.4148	0.0000	0.3397	0.3268	0.6171	0.3049	0.0501	0.4830
Gli2	0.0002	0.0003		0.8839	0.1219	0.3546	0.9017	0.0000	0.5745	0.5847	0.6784	0.6624	0.0019	0.0118
Ptc1	0.4152	0.4296	0.8839		0.0001	0.5525	0.4151	0.5973	0.0002	0.0060	0.0012	0.0559	0.7872	0.1356
Hip	0.5587	0.4950	0.1219	0.0001		0.7176	0.9003	0.4119	0.0002	0.0277	0.0122	0.1319	0.6367	0.0241
ADAM12	0.9729	0.8461	0.3546	0.5525	0.7176		0.4206	0.5736	0.9703	0.8859	0.1454	0.8203	0.0005	0.1165
Agpt4	0.3807	0.4148	0.9017	0.4151	0.9003	0.4206		0.5514	0.4144	0.8708	0.7978	0.9612	0.6044	0.6937
BRAK	0.0000	0.0000	0.0000	0.5973	0.4119	0.5736	0.5514		0.5158	0.3861	0.9763	0.3004	0.0035	0.2187
Fbn2	0.3023	0.3397	0.5745	0.0002	0.0002	0.9703	0.4144	0.5158		0.0470	0.0234	0.0561	0.8868	0.0244
Fgf5	0.2993	0.3268	0.5847	0.0060	0.0277	0.8859	0.8708	0.3861	0.0470		0.0364	0.0058	0.8836	0.4764
Hes1	0.6328	0.6171	0.6784	0.0012	0.0122	0.1454	0.7978	0.9763	0.0234	0.0364		0.4232	0.2632	0.0219
HSD11b1	0.2738	0.3049	0.6624	0.0559	0.1319	0.8203	0.9612	0.3004	0.0561	0.0058	0.4232		0.6490	0.2955
Igfbp6	0.0285	0.0501	0.0019	0.7872	0.6367	0.0005	0.6044	0.0035	0.8868	0.8836	0.2632	0.6490		0.0416
Timp3	0.4680	0.4830	0.0118	0.1356	0.0241	0.1165	0.6937	0.2187	0.0244	0.4764	0.0219	0.2955	0.0416	

benign non-reactive

n=11	Shh	Gli1	Gli2	Ptc1	Hip	ADAM12	Agpt4	BRAK	Fbn2	Fgf5	Hes1	HSD11b1	Igfbp6	Timp3
Shh		0.0000	0.0004	0.9577	0.0006	0.8831	0.0000	0.5134	0.0612	0.6376	0.9206	0.3792	0.0160	0.0720
Gli1	0.0000		0.0009	0.9129	0.0010	0.7177	0.0000	0.4749	0.0663	0.7542	0.8785	0.4173	0.0147	0.0574
Gli2	0.0004	0.0009		0.4834	0.0000	0.3179	0.0161	0.8394	0.0132	0.7386	0.5634	0.3181	0.0007	0.0160
Ptc1	0.9577	0.9129	0.4834		0.2211	0.9538	0.9628	0.5339	0.3031	0.0038	0.8076	0.9541	0.4249	0.0060
Hip	0.0006	0.0010	0.0000	0.2211		0.4308	0.0124	0.7014	0.0088	0.5429	0.5539	0.2976	0.0011	0.0027
ADAM12	0.8831	0.7177	0.3179	0.9538	0.4308		0.2738	0.0290	0.4818	0.9266	0.2392	0.6678	0.2868	0.9905
Agpt4	0.0000	0.0000	0.0161	0.9628	0.0124	0.2738		0.2678	0.1826	0.7624	0.8606	0.6322	0.0702	0.0824
BRAK	0.5134	0.4749	0.8394	0.5339	0.7014	0.0290	0.2678		0.6084	0.3864	0.0694	0.7152	0.5852	0.7693
Fbn2	0.0612	0.0663	0.0132	0.3031	0.0088	0.4818	0.1826	0.6084		0.6730	0.0852	0.1466	0.0024	0.0670
Fgf5	0.6376	0.7542	0.7386	0.0038	0.5429	0.9266	0.7624	0.3864	0.6730		0.4842	0.8804	0.3837	0.0292
Hes1	0.9206	0.8785	0.5634	0.8076	0.5539	0.2392	0.8606	0.0694	0.0852	0.4842		0.7162	0.0505	0.7229
HSD11b1	0.3792	0.4173	0.3181	0.9541	0.2976	0.6678	0.6322	0.7152	0.1466	0.8804	0.7162		0.3431	0.5408
Igfbp6	0.0160	0.0147	0.0007	0.4249	0.0011	0.2868	0.0702	0.5852	0.0024	0.3837	0.0505	0.3431		0.0313
Timp3	0.0720	0.0574	0.0160	0.0060	0.0027	0.9905	0.0824	0.7693	0.0670	0.0292	0.7229	0.5408	0.0313	

Figure 6. Analysis of reactive stroma and hedgehog signaling in human prostate tissue. The relationship of reactive stroma and Hh signaling was analyzed in prostate using Pearson product-moment correlation. The samples were divided into 4 groups according to benign/tumor and reactive/non-reactive. The numbers listed are correlation p values. Values less than 0.05 are highlighted in red. All correlations in red are positive correlations (data not shown).